Observation of W and Z boson candidates with the CMS experiment

Emanuele Di Marco for the CMS Collaboration

"La Sapienza" Università di Roma and INFN Roma, p.le Aldo Moro n. 2, 00185 Roma, Italy

We present the first observation of W and Z boson candidates in muon and electron decay channels in 198 nb^{-1} pp collisions at $\sqrt{s} = 7$ TeV, using the CMS detector at the LHC.

1 Introduction

The production of W and Z bosons decaying to charged leptons is an important process to measure at the LHC: it can be used to validate lepton reconstruction and identification to be used in future analyses, a precision test of perturbative QCD and the parton distribution functions of the proton (PDFs), a possible estimator of integrated luminosity for proton collisions, and the first electroweak process to be observed at the LHC. At the LHC, QCD predictions, in next-to-next-to leading order (NNLO) in the strong coupling α_s, exist for the matrix elements describing inclusive W and Z production. The cross section can be predicted with a few percent uncertainty. The production of the W and the Z in hadron collisions has been measured at several previous experiments over a range of collision energies, and Standard Model predictions have been observed to agree well with them.

2 Measurement of the $W \rightarrow \mu\nu$ and $Z \rightarrow \mu^+\mu^-$ yield

$W \rightarrow \mu\nu$ events are characterized by a high-p_T isolated muon, together with a signicant amount of missing transverse energy ($\not{E}_{\mathrm{T}}$), due to the presence of a neutrino in the final state that escapes undetected. Events with high-p_T muons are recorded online using the Level-1 muon trigger and the high-level trigger (HLT), which require information from the muon chambers (Level-1, HLT) and the inner tracker (HLT). A trigger path with an HLT threshold of $p_T > 9$ GeV in the $|\eta| < 2.1$ region is chosen as the baseline of the analysis. The muon must be identified by two different algorithms, one that starts from inner tracker information ("tracker muons"), and another one that starts from segments in the muon chambers ("global muons"). Quality cuts on the inner track and on the results of the global muon fit is applied to reduce the contamination from muons produced in decays in flight of hadrons and from punch-through. We demand the presence of at least two levels of muon stations to suppress candidates which are unable to penetrate deeply in the iron yoke of CMS [1]. A full reconstruction of the W system is not possible but a mass reconstruction in the transverse plane can be performed from the measured $\not{E}_{\mathrm{T}}$ and the muon momentum. This transverse mass is defined as: $M_T =$

$\sqrt{2p_T(\mu)\not{E}_T(1-\cos(\Delta\phi_{\mu,\not{E}_T}))}$, where $\Delta\phi_{\mu,\not{E}_T}$ is the azimuthal angle between muon and $\not{E}_T$ directions. The resulting M_T distribution exhibits the characteristic shape of the W Jacobian peak. Events with two high p_T muons are rejected to minimize the contribution of Drell-Yan events. The muons are required to be isolated discarding the ones with high activity in a cone around the muon in the inner tracker, electromagnetic calorimeter (ECAL) and hadronic calorimeter (HCAL). After the selection 1254 events are selected. The main sources of background are QCD events with muons coming from decays of b-hadrons, with a smaller contribution of muons from long-lived meson decays. The remaining background is $Z \to \mu^+\mu^-$, with one muon beyond the detector acceptance (3% background), $Z \to \tau^+\tau^-$ and $W \to \tau\nu$ events (2% contamination). The $t\bar{t}$ background is negligible (0.3%). The $W \to \mu\nu$ signal yield is extracted from a binned likelihood fit to the observed M_T distribution. Figure 1 (a) shows the fit to the observed M_T spectrum, together with the different templates used. The measured yield is $N_W = 818 \pm 27$ (stat.). $Z \to \mu^+\mu^-$ events are characterized by the presence of two high-p_T isolated muons forming a di-muon system with an invariant mass consistent with the Z boson mass. The expected background is very low, and therefore it is estimated from Monte Carlo. Di-muon pairs with opposite charge are selected with looser requirements than the one described for the W case if their invariant mass satisfies $60 < m_{\mu\mu} < 120$ GeV. We select 77 events: the invariant mass of these pairs is shown in Figure 1 (b). Data are compared with the Monte Carlo NLO expectations for this luminosity. The background, dominated by QCD, $t\bar{t}$ and $Z \to \tau^+\tau^-$ events, is negligible ($\approx 0.3\%$).
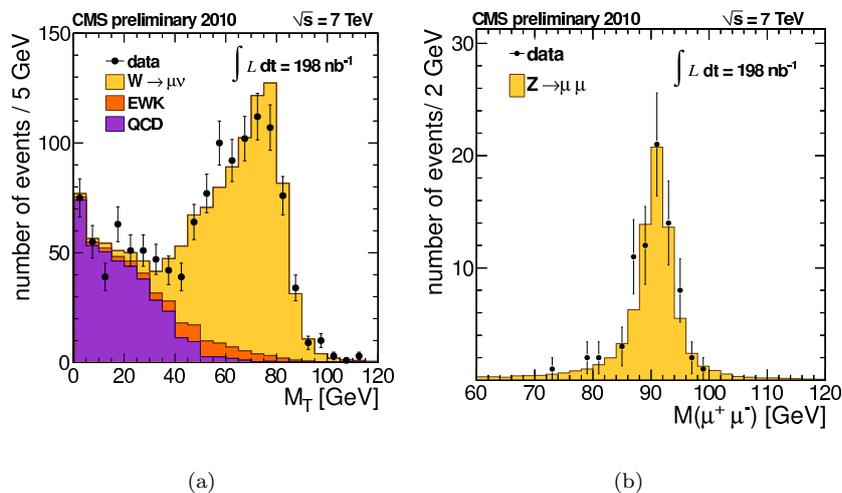

(a)   (b)

Figure 1: (a) Fit to the m_T spectrum of W candidates (black points) together with the templates for the different processes. (b) Invariant mass distribution of the selected $Z \to \mu^+\mu^-$ candidates in data superimposed to the MC expectation.
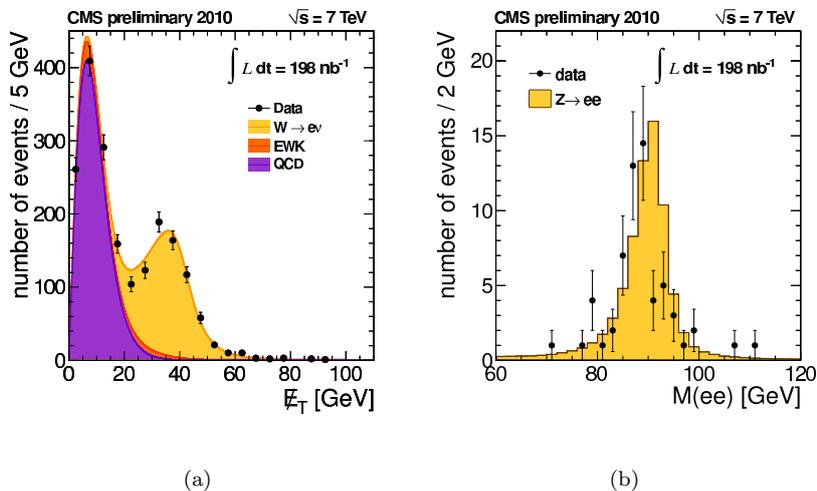
Figure 2: (a) Fit to the $\not{E}_T$ spectrum of W candidates (black points) together with the templates for the different processes. (b) Invariant mass distribution of the selected $Z \to e^+e^-$ candidates in data superimposed the MC expectation.

3 Measurement of the $W \to e\nu$ and $Z \to e^+e^-$ yield

Electrons are identified in the CMS detector as clusters of ECAL energy deposits matched to tracks from the silicon tracker. The ECAL covers the pseudorapidity range $|\eta| < 3.0$. Electron candidates are selected online from events that: pass a "Level 1" (L1) trigger filter, evaluated by customized hardware, which requires a coarse-granularity region of the ECAL to have $E_T > 5$ GeV; and that subsequently pass a "High Level Trigger" (HLT) software filter, requiring an ECAL cluster with $E_T > 15$ GeV, using the full granularity of the ECAL and E_T measurements calibrated to offline precision. Electron candidates require an ECAL cluster with $E_T > 20$ GeV, in the ECAL acceptance. ECAL clusters are required to match tracks using an algorithm which accounts for possible energy loss due to bremsstrahlung in the tracker layers. Particles misidentified as electrons are suppressed by: requiring the track trajectory to geometrically match the ECAL cluster; by limiting the amount of HCAL energy measured in a cone radius of $\Delta R < 0.15$ around the ECAL cluster direction; and by requiring a narrow ECAL cluster width in η. Photon conversions rejection criteria are also applied. Those identified electrons are required to be isolated requiring low activity around their direction in the tracker, ECAL and HCAL detectors. W candidates are required to have one electron, with ECAL cluster $E_T > 20$ GeV, satisfying the described identification criteria. Z events are suppressed rejecting events with a second electron candidate. This selection results in 1931 candidate events in 198 nb^{-1}. Remaining backgrounds consist of QCD di-jet events, prompt high-E_T photons, Z events, and $W \to \tau\nu$ events. The first two sources are characterized by small intrinsic $\not{E}_T$, and can be separated from $W \to e\nu$ signal from an analysis of the $\not{E}_T$ distribution. The last two sources can be modeled successfully by Monte Carlo simulation. The $W \to e\nu$ signal is extracted via an unbinned maximum likelihood fit to the $\not{E}_T$ distribution. Figure 2 (a) shows

the $\not{E}_T$ distribution of $W \to e\nu$ candidates and the results of the likelihood fit. The $W \to e\nu$ signal yield estimated from the fit is 799.7 ± 30.6 (stat.) events. Z candidates are required to have two electrons, with ECAL cluster $E_T > 20$ GeV, satisfying the criteria described above, but with a looser operating point than the W selection for electrons. The invariant mass of the electron pair is required to be between 60 and 120 GeV. This selection results in 61 candidate events in 198 nb^{-1}. Simulations of QCD di-jets estimate a background of much less than one event. Figure 2 (b) shows the mass distribution of $Z \to e^+e^-$ candidates with predictions from simulation superimposed. The data exhibit an energy scale shift relative to simulation of 1%.
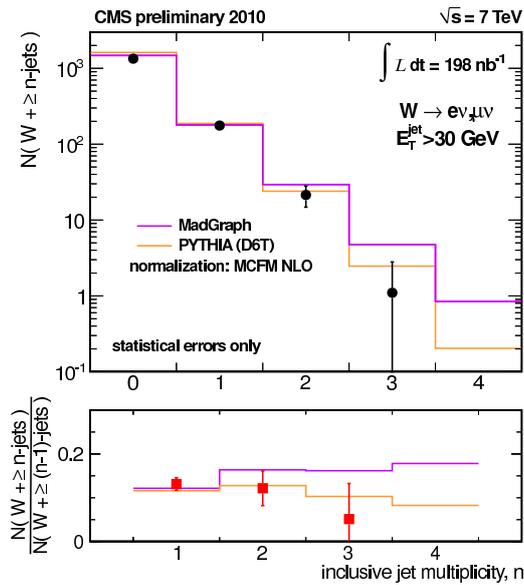

Figure 3: Number of $W \to \ell\nu$ events ($\ell = e, \mu$) containing n jets above threshold or more (top plots) and ratio $N(W \to \ell\nu,\, n \text{ jets})/N(W \to \ell\nu,\, \geq (n-1) \text{ jets})$ (bottom plots).

4   Production of W, Z associated with jets

We study the production of hadronic jets along with W bosons reconstructed in leptonic decay modes. The lepton selections are identical to those described in Section 2 for $W \to \mu\nu$ and in Section 3 for $W \to e\nu$. Hadronic jets are reconstructed by clustering charged and neutral hadrons and photons. The infrared-safe Anti-kt [2] jet clustering with a cone radius of $\Delta R = 0.5$ is used. We consider jets within the tracker acceptance $|\eta| < 2.5$ with an energy threshold of $E_T > 30$ GeV. Events are classified according to the number of jets above threshold in an inclusive way: the jet multiplicity bin n gathers events containing n jets or more in addition to the lepton. The $t\bar{t}$ background is sizable in jet-multiplicity bins $n \geq 3$. In the electron channel, the ratio of $t\bar{t}$ background with respect to the signal is fixed to the expectation from Monte Carlo simulation. Figure 3 presents the results $N(W \to \ell\nu + \geq n \text{ jets})$ as a function of the inclusive jet multiplicity n. Electron and muon results are combined. The rate of high

E_T jets is sensitive directly to the matrix element of the hard scattering at the parton level. Here we compare the data with predictions obtained with two different generators, PYTHIA [3] and MADGRAPH [4]. All Monte Carlo predictions are normalized to the NLO inclusive cross section prediction obtained with the MCFM generator.

5   Conclusions

First observation of W and Z (γ^*) bosons have been made using approximately 198 nb^{-1} of data taken with the CMS detector at the LHC. In addition, the W production in association with jets have been measured. Within large statistical uncertainties, no disagreements with the predictions of the Standard Model have been observed.

References

[1] R. Adolphi *et al.* [CMS Collaboration], "The CMS experiment at the CERN LHC," JINST **3** (2008) S08004.

[2] M. Cacciari, G. P. Salam and G. Soyez, "The anti-k_t jet clustering algorithm," JHEP **0804**, 063 (2008)

[3] T. Sjostrand, S. Mrenna and P. Z. Skands, "PYTHIA 6.4 Physics and Manual," JHEP **0605** (2006) 026

[4] F. Maltoni and T. Stelzer, "MadEvent: Automatic event generation with MadGraph," JHEP **0302** (2003) 027